Arabian Journal for Science and Engineering (2023) 48:9439–9447
https://doi.org/10.1007/s13369-022-07504-y

RESEARCH ARTICLE-PETROLEUM ENGINEERING

Improved Stabilization of Sulfated Zirconia by Molybdenum: Synergy of Metal Sites and Acid Sites in the *n*-Hexane Hydro-Isomerization

Sahar Raissi[1] · **Mohamed Kadri Younes**[1]

Received: 8 December 2021 / Accepted: 17 November 2022 / Published online: 21 December 2022

Abstract
Hydrogen has a crucial role in preventing deactivation of sulfated zirconia (ZS). Hydro-isomerization of*n*-hexane is carried out with (ZS) doped with molybdenum mechanically mixed platinum supported by alumina. This catalyst presents an important improvement of the activity and stability compared to the non-doped one. At 443 K, doped and non-doped catalysts present, respectively, the activities 3×10^{-8} and 2×10^{-8} molL^{-1} g^{-1}. By increasing temperature, while doped catalyst activity rises to 2.6×10^{-7} molL^{-1} g^{-1}, the activity of the non-doped one drops to 3.4×10^{-9} molL^{-1} g^{-1}. Characterization of solids by XRD shows the presence of ZrO_2 tetragonal phase in all the solids. Raman spectroscopy confirms this finding. UV–Visible spectroscopy shows influence of calcination temperature on molybdenum geometry. At low temperature (673 K), specific surface area is developed ($S_{BET} = 144$ m^2 g^{-1}) and the metal is in tetrahedral geometry as MoOx. Those sites enhance acidity and generate acid sites utilizing an atomic-scale spillover effect of H_2 on platinum particles.

Keywords H_2 spillover · Tetrahedral · Octahedral · Molybdenum

1 Introduction

Crude petroleum is naturally occurring as hydrocarbons mixture of various molecular weights. Considering its origin coming from zooplankton and algae transformation by burying underneath in intense heat and pressure, petroleum is characterized by complex structure and multiple components [1]. It includes*n*-alkanes, cyclo-alkanes and polycyclic aromatic hydrocarbons and asphaltene constituted of heteropolycyclic. According to recent OPEC report [2], the demand of gasoline, issued from petroleum, will mark an increase of 17.6 mb/d in the period 2020–2045 mainly in non-OECD countries because of the road transportation and aviation sectors. An expanding middle class and a high growth rate population drive this development. The C5–C10 fraction issued from oil distillation gives the base of gasoline used as fuel in spark-ignited internal combustion engines. Optimum motor's function requires an important value of Octane Number (RON), which traduces the resistance of gasoline to knocking. Moreover, researches [3, 4] show that rising (RON) of gasoline from 95 to 100 ensures gain of consumption reaching 4.4% and reduces emission of CO_2 and hydrocarbons. Since the fraction, issued from crude oil distillation, is largely formed of straight chains, it must be mixed with additives that enhance this rate like ethyltertibutylether and other oxygenated derivate, branched alkanes, benzene, xylene, toluene and other aromatics [5, 6]. Isopentane has, nearly 30 times higher, Octane Number value than*n*-pentane. Similarly, the hexane isomer, 2,2-dimethylbutane has an octane number of 105 versus 31 for *n*-hexane [7]. Thus, to be in harmony with requirements of environment respect, *n*-alkane isomerization is a process that is more and more growing and gaining importance in the refining field [8]. It ensures an upgrading of gasoline composition to make it more eco-friendly. However, the dilemma of a large use of this refining process still up today finding an efficient catalyst at low temperature to avoid cracking and favoring di-branched alkane [9]. Acid and bi-functional catalysts can ensure this reaction activation at very low temperature. Sulfated zirconia (ZS) is one of the most attractive catalyst of this reaction [10, 11]. In general, ZS has attracted researchers' attention because of its super-acid character from one hand [12]. From

✉ Sahar Raissi
Sahar.raissi@fst.utm.tn

Mohamed Kadri Younes
Mohamedkadri.younes@fst.utm.tn

[1] Laboratory of Material Chemistry and Catalysis, University of Tunis El Manar, Tunis, Tunisia

the other hand, zirconia provides remarkable surface properties mainly hardness and high thermal stability [13], but this catalyst suffers from rapid deactivation. The mechanism of *n*-alkane isomerization on acid solids proceeds via carbenium ion formation, which is intermediate for both isomerization and cracking [10]. Hydrogen can be used to react with the carbenium and favor isomerization instead of cracking. Thus, it protects catalyst from coke deposing [14]. Adjunction of metal, noticeably noble ones, can also improve catalyst stability by preventing coke deposition [11, 15]. But, as reported by Ben Hammouda and Ghorbel [16], use of platinum during hydro-isomerization of*n*-hexane provokes sulfur loss and causes deactivation of the catalyst by acidity decrease. Zirconium modified by molybdenum showed good properties in hydro-isomerization [17]. In this work, we studied the reaction of *n*-hexane hydro-isomerization by sulfated zirconia modified by molybdenum (ZSMo) and mechanically mixed to platinum supported on alumina. The choice of molybdenum is dictated by its involvement in spillover phenomenon which can affect hydro-isomerization mechanism [18, 19]. Sol–gel method coupled to super-critical conditions of solvent evacuation was adopted for solid preparation. The focus was put on the calcination temperature effect on the structuration of the final solid and the development of active sites. A comparison between catalytic performances of doped and non-doped solids was carried out.

2 Experiments

2.1 Catalysts Preparation

The sulfated Mo doped zirconia catalysts were prepared by sol–gel method coupled to supercritical drying. First, a quantity of zirconium propoxide (ALDRICH, 70% in propanol) was dissolved in 1-propanol (ACROS 99%). Then, a quantity of concentrated sulfuric acid (ACROS 96%), corresponding to nS/nZr = 0.5, followed by a quantity of molybdenum acetylacetonate (ACROS 97%) corresponding to nMo/nZr = 0.1, were added. The sol was kept under constant stirring. Gel formation is immediate and occurs by pure water adjunction. Obtained gel was introduced, without aging, into an autoclave. It was dried under supercritical conditions of the solvent (536.6 K, 51 bar). The obtained aerogel was ground and calcined under oxygen during 3 h at various temperatures in the range 673 and 973 K. Solids were designated as: ZSMoH for le one calcined at 923 K and ZSMoL for the one calcined at 673 K.

Platinum supported by alumina was prepared by wet impregnation of commercial alumina (Aldrich, particular size 1 μm) by 6% in mass of sodium hexachloroplatinate (IV) (Aldrich 98%). Impregnated was dried for 24 h at 100 °C. After that, it was reduced for 6 h under hydrogen at 220 °C.

2.2 Catalysts Characterization

The XRD patterns were collected on an automatic Philips Panalytical diffractometer using Cu kα radiation (k = 1.54056 Å) and Ni monochromator in the range $2\theta = 20°$–$60°$ with a scanning speed 2°/min. The reticular distances calculated were compared to those given by the Joint Committee on Powder Diffraction Standards (JCPDS # 80–2155).

Scanning electronic microscopy images were obtained using Philips Tecnai G2 F30 S-Twin.

Porosity and surface area were measured by N_2 adsorption at 77 K via Micromeritics apparatus ASAP 2000, monitored by a computer. Before adsorption, samples were degassed for 4 h under vacuum at 473 K.

IR spectra were recorded at resolution 2 cm^{-1} with a PerkinElmer FTIR spectrophotometer over a range of 4000–400 cm^{-1} in the transmission mode on samples mixed with KBr (2 mg in 200 mg).

UV–Visible spectra were collected on a PerkinElmer spectrophotometer lambda 45 coupled to an integration sphere RSA-PE-20 in the range 200–900 nm with a speed of 960 nm min^{-1} and an aperture of 4 nm.

Raman spectra was performed on a Jobin Yvon Labram 300 Raman spectrometer equipped with a confocal microscope, a CCD detector, and a He–Ne laser source (λ = 633 nm). Raman spectra of the samples, used in the powder form, were recorded at ambient temperature in the 200–1500 cm^{-1}.

2.3 Catalytic Test

The catalysts used on the catalytic test consisted of 0.1 g of sulfated zirconia doped with molybdenum calcined at different temperatures mechanically mixed with 0.01 g of platinum dispersed on alumina (6%).

The *n*-hexane hydro-isomerization was performed by the contact of *n*-hexane (0.027 bar) diluted in H_2 (30 cm^3 min^{-1}) with the catalyst in U-shaped tubular continuous flow reactor at atmospheric pressure and 423, 443, 473 and 493 K. The catalyst, after a treatment of 1 h at 673 K under N_2 (30 cm^3 min^{-1}), remained in each temperature 2 h. Each 15 min, an on-line chromatography unit, with a squalane on spherosil column, ensured the analysis of reactant and reaction products [20, 21]. Medium activity, at each temperature, was reported as a function of reaction temperature.

Activity is calculated by the following formula (1):

$$A_c = \frac{dn_p}{dt} = \frac{T_b}{T} \times \frac{D_t}{V_b} \times n_p \quad (1)$$

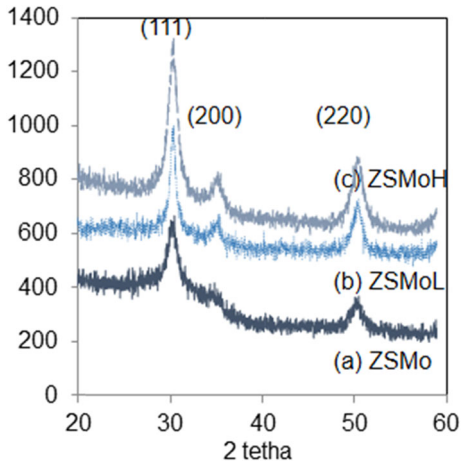

Fig. 1 XRD patterns of Mo promoted sulfated zirconia **a** non-calcined, **b** calcined at 673 K, calcined at 923 K

With

$$n_p = \sum_{k=1}^{6} \sum_{i} \frac{k}{6} s_i a_i \tag{2}$$

n_p: Number of mol of the product p, k: Number of carbon in the product I. s_i: Coefficient of proportionality of the product i.

a_i: Surface of the pic relative to the product i.

T: Room temperature.

T_b: Injection loop temperature, $T_b = T$.

D_t: Flow, $D_t = 30$ cm^3/min.

V_b: Loop volume, $V_b = 0, 5$ cm^3

Selectivity of isomerization is calculated by (3)

$$S_p(\%) = \frac{N_{RP}}{N_{tR}} \times 100 \tag{3}$$

N_{RP}: Number of mole of reactant transformed in product.

N_{tR}: Total number of mole of transformed reactant.

3 Results and Discussion

Figure 1 regroups aerogels XRD patterns as function of calcination temperature. The two calcined solids develop the ZrO_2 tetragonal phase characterized by the peaks situated at $2\theta = 30.36°, 35.16°, 50.46°$ (JCPDS # 80-2155). It seems that the development of this phase, at calcination temperature as low as 673 K, is due to the molybdenum doping and to drying under supercritical conditions. In fact, a same phenomenon was noted in the case of solids based on zirconia doped with other transition metals like cobalt and chromium [20, 21].

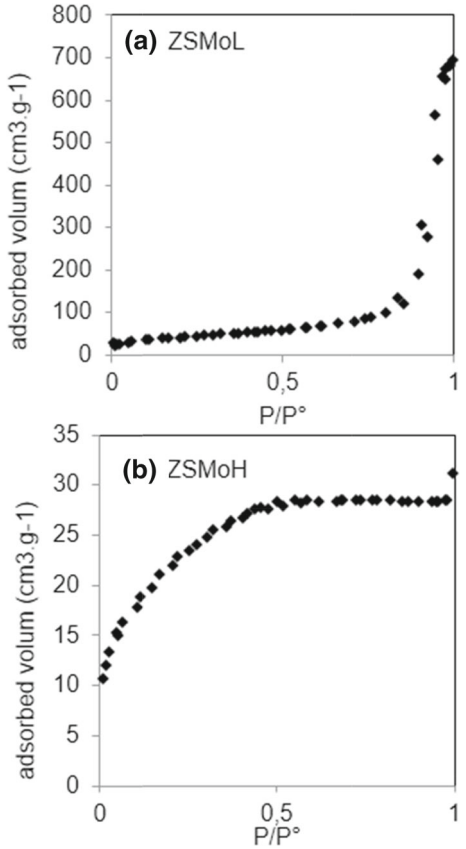

Fig. 2 Isotherms of N_2 adsorption and desorption at 77 l on Mo promoted sulfated zirconia **a** calcined at 673 K, **b** calcined at 923 K

The same preparation protocol of non-promoted sulfated zirconia did not induce the stabilization of this phase at such low temperature [15].

No crystalline phase relative to molybdenum or its oxides is observed which reveals a good dispersion of the metal on the surface of the solid and its insertion in the lattice of the zirconium structure.

N_2 physisorption was carried out at 77 K. It gave an isotherm of type Iva for the solid calcined at 673 K and hysteresis of type H1 [22] (Fig. 2a). We can conclude that this solid is mesoporous with spherical particles of uniform size. The evaluation of the mesoporous volume by t-plot estimates it to 0.9 cm^3 g^{-1}. The specific surface area is estimated to 144 m^2 g^{-1}.

Calcination temperature affects deeply the morphology of this solid. When it reaches 923 K, isotherm becomes of type Ia [22] (Fig. 2b). However, we note the presence of a growing adsorbed volume at high pressures that could result from superposition of types I and II of isotherms. Specific surface area is reduced to 75 m^2 g^{-1} and the micro-porous volume to 0.001 cm^3 g^{-1}. It seems that the texture is very destroyed by calcination and only a small number of micropores have been preserved. This phenomenon could be related to departure of

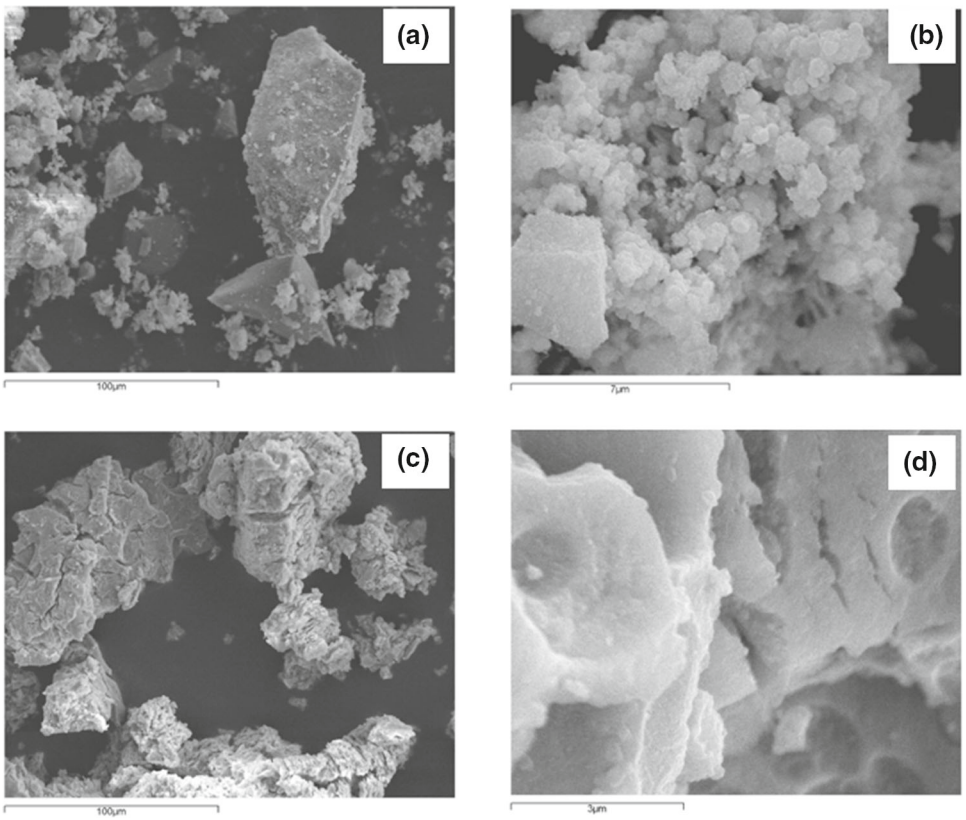

Fig. 3 SEM of Mo promoted sulfated zirconia calcined at 673 K **a** × 550, **b** × 8000 and calcined at 923 K, **c** × 550, **d** × 15,000

sulfate groups as it is reported by Mejri et al. [15]. High calcination temperature favors sulfate groups decomposition and sulfur loss.

Scanning electronic micrographs of the two catalysts confirm the differences concluded from N_2 physisorption. While the solid calcined at 673 K consists of small spherical particles of glomerular appearance (Fig. 3a and b), the solid calcined at 923 K exhibit flat particles on irregular shape and size (Fig. 3c and d) with the presence of large creates and holes on a dense volume.

IR spectroscopy (Fig. 4) also confirms the deep affectation of molybdenum doped sulfated zirconia by calcination temperature. In fact, the peak situated at 1650 cm^{-1} assigned to δ_{HOH} of water adsorbed [23] is weakened by calcination and this is related to the change of the porosity. Besides, the peak at 3500 cm^{-1} relative to hydroxyl group has almost disappeared at 923 K of calcination. An alteration of the Brönsted acidity can be expected. A similar phenomenon was observed in the case of doping sulfated zirconia with chromium [20].

Likewise, the sulfate groups characteristic of inorganic chelating bidentate sulfate, assigned to asymmetric and symmetric stretching frequencies of bands relative to $\nu_{(S-O)}$ and situated at 1020, 1160 and 1250 cm^{-1} are widely affected by the calcination temperature [24]. They are likely to completely disappear at 923 K. The most important observation on the spectra of the catalyst ZSMoH is the absence of

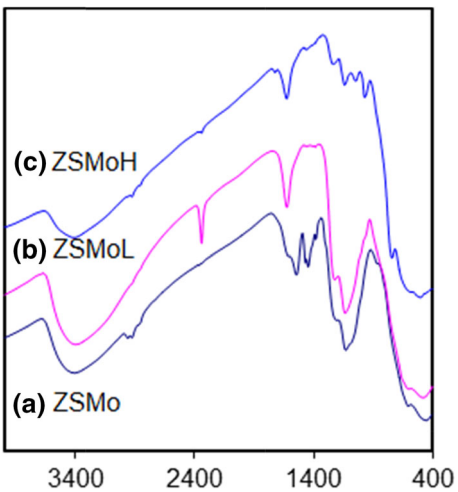

Fig. 4 IR spectra of Mo promoted sulfated zirconia **a** non-calcined, **b** calcined at 673 K, **c** calcined at 923 K

the band situated at 1380 cm^{-1}, and the band situated at 1445 cm^{-1} characteristic of active sulfate group [24]. In fact, those bands are, respectively, associated to $\nu_{S=O}$ and covalently bonded S=O which display Lewis acid sites in sulfated zirconia samples [25]. The importance of those bands is reported by many authors as sites enhancing the activity in *n*-alkanes isomerization reactions. Therefore, absence in

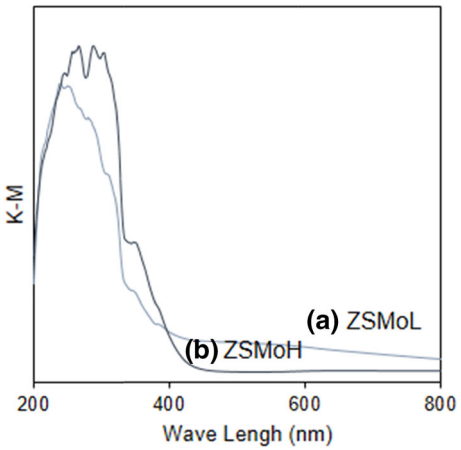

Fig. 5 UV–Visible spectra of Mo promoted sulfated zirconia **a** calcined at 673 K, **b** calcined at 923 K

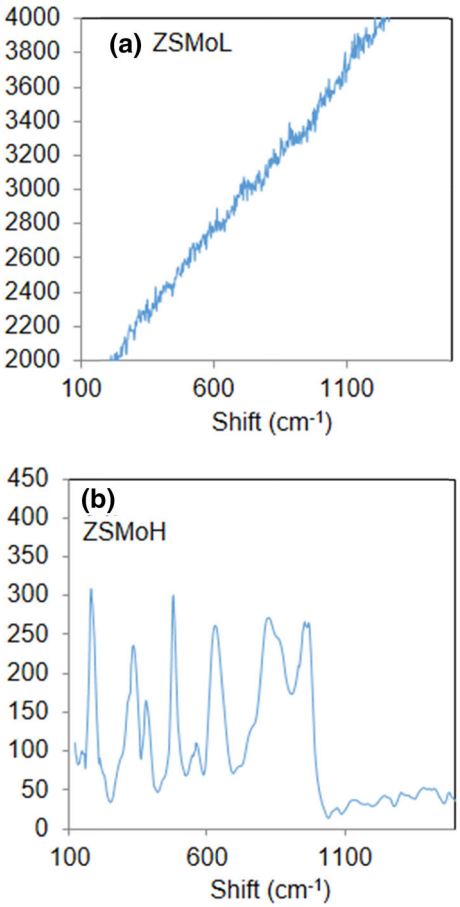

Fig. 6 Raman spectra of Mo promoted sulfated zirconia **a** calcined at 673 k, **b** calcined at 923 K

spectra of calcinated solids suggests that the active sites in those catalysts are almost due to the molybdenum species.

Moreover, all the spectra show two bands at 467 and 585 cm^{-1} corresponding to $1A_{2u}$ and $2E_u$ vibration in ZrO_2 tetragonal which is confirmed by XRD results [26]. Those peaks are bad resoluted due to the bad crystallinity of the solids.

Besides, at high calcination temperature, a peak situated at 981 cm^{-1} rises due to Mo=O stretching mode in octahedral symmetry [27].

Figure 5 illustrates UV–visible spectra. It shows evolution of molybdenum coordination due to calcination temperature increase. The spectrum of the solid calcinated at 673 K presents a pic at 245 nm characteristic of tetrahedral molybdenum (VI) that disappears completely when the calcination temperature reaches 973 K. At this temperature, a pic situated around 305 nm and characteristic of octahedral molybdenum rises [28]. In fact, octahedral molybdenum is known to occur as polymeric oxomolybdic species and cannot exist as isolated species contrarily to tetrahedral molybdenum that can be found isolated on the surface of the solid [28]. Increasing calcination temperature seems to favorite polymerization of oxomolybdic species.

The characteristic band relative to charge transfer from the valence band (O 2p) to the conduction band (Zr 4d): O^{2-} (2p) Zr^{4+} (4d) is situated at 213 nm which confirm the tetragonal structure of zirconia [29].

Figure 6a and b represents Raman spectra of the solids ZSMoH and ZSMoL. The later, calcined at low temperature, does not show any peak may be because well dispersion of amorphous tetrahedral molybdenum on its surface [30]. On the spectra of the solid calcined at high temperature, we detect easily peaks characteristic of A1g and Eg vibrational modes for tetragonal zirconia at 477, 638 and 618 cm^{-1} [25, 31]. We also note the presence of a doublet at 180–190 due to Ag mode and band at 222 cm^{-1} due to Bg mode of vibration in monoclinc ZrO_2 and the band at 334 cm^{-1} due to monoclinic ZrO_2 that seems to start to appear in very small quantity because XRD does not revealed it [25, 31]. No peak relative to sulfate vibration is detectable [16]. The peaks between 750 and 1000 cm^{-1} can be assigned to range of molybdenum oxidation states with several phases of oxide presence including octahedral Mo (VI) species in particular the bands situated at 819 and 990 cm^{-1} are assigned to more pronounced pure phase of MoO_3 [25, 32–34].

Catalytic performances of the two solids are studied in *n*-hexane hydro-isomerization. Catalytic tests are performed in presence of pure molybdenum sulfated zirconia, or a mechanical mixture of this catalyst with an equal mass of platinum deposited on alumina Pt/Al_2O_3 6%. Platinum is mixed with sulfated zirconia in order to avoid deactivation [34]. Figure 7 gathers catalytic activities of ZS, ZSMoL and ZSMoH. It shows that molybdenum improves catalytic activity of ZS. While undoped catalyst deactivates during the time even though temperature increase, doped ones mark jump in activity when temperature increases. It indicates a good stability of

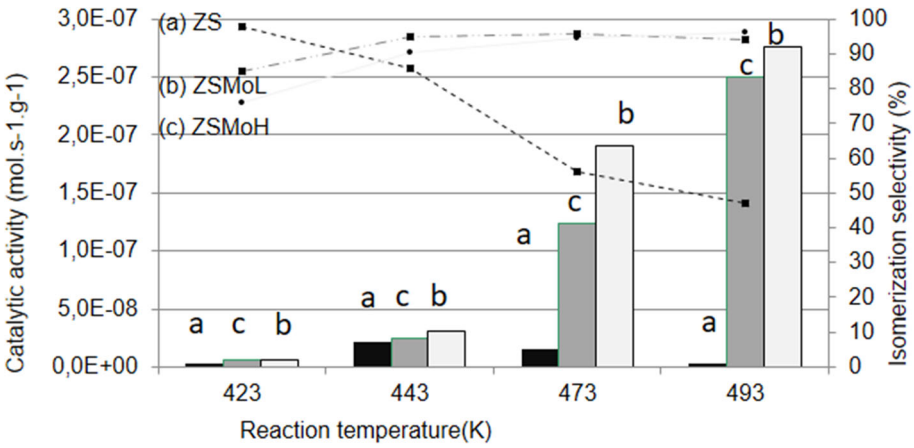

Fig. 7 Isomerization activity (histogram) and stability (curve) versus reaction temperature of mixed Pt/Al2O3 with **a** non-promoted sulfated zirconia ZS and Mo sulfated zirconia, **b** calcined at 673 K or **c** calcined at 923 K. $P = 1$ atm; H2 flow = 30 mL/min; Pc6 = 0.027 bar; m 0.1 g

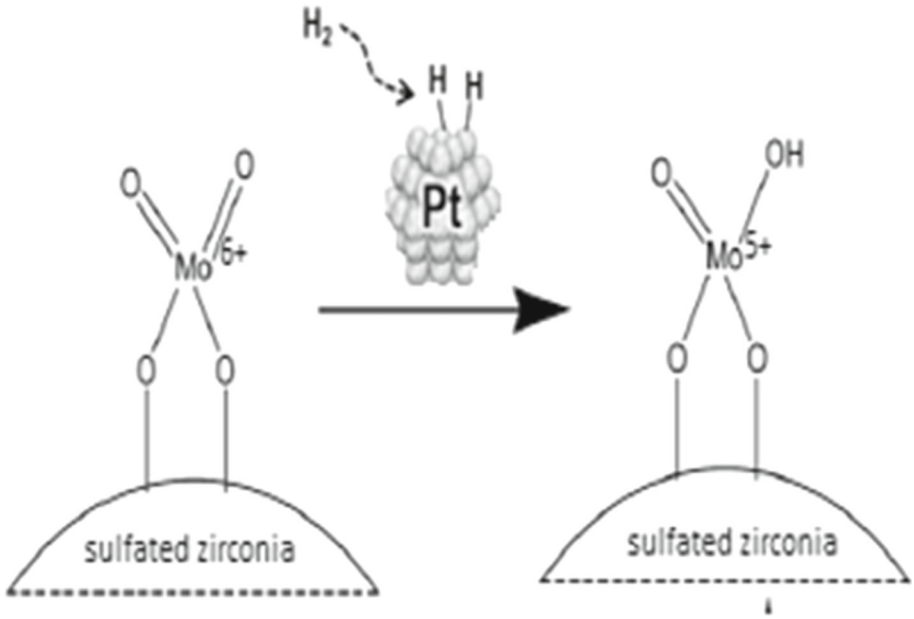

Fig. 8 Proposed pathway of interaction of tetrahedral molybdenum with H_2 spilled over platinum particles implying generation of Bronsted acid site on MoO*x* metallic sites

those solids. In those conditions, ZSMoL is the most active. Test carried out with only Pt/Al_2O_3 showed that this solid is completely inactive in the investigated range of temperature. It seems that synergy between the two metals takes place and affects reaction mechanism. Table 1 regroups performances of some catalysts of*n*-hexane isomerization over different conditions.

ZS is known as super acid catalyst that was largely studied in light*n*-alkane isomerization. However, it suffers from rapid deactivation. Hence, to increase its stability, this catalyst was mixed with Pt/Al_2O_3 in order to clean acid sites and inhibit coke deposition in the work of Méjri et al. [34]. However, Ben Hammouda et al. [16] found that platinum use can present the drawback of deactivation because it causes sulfate loss and thus stability decreases. In the current study, we try to get around this weakness by adding molybdenum as doping metal to sulfated zirconia. Actually, it can be observed that doped catalysts develop better activity and more stability than undoped ones. This catalyst has a different catalytic behavior. While pure sulfated zirconia is quickly deactivated and cannot be regenerated by reaction temperature increase, doped one is stable and present higher activity when increasing reaction temperature.

The introduction of this metal affects the reaction mechanism. H_2 spillover seems to be responsible of the catalyst stability. However, it is important to note that occurrence of this phenomenon is tightly related to the nature of molybdenum species. According to Prins [37], when mixing platinum tetrahedral molybdenum, a synergy between the two metals induces an important H_2 uptake due to spillover occurring at temperature as low as 223 K. H_2, the carrier gas, interacts with tetrahedral molybdic species to spill over and form (MoO_x–H_y^+) generating protonic sites responsible of the continuity of catalyst activity. Spillover of hydrogen from metal particles can lead to its reduction and apparition of

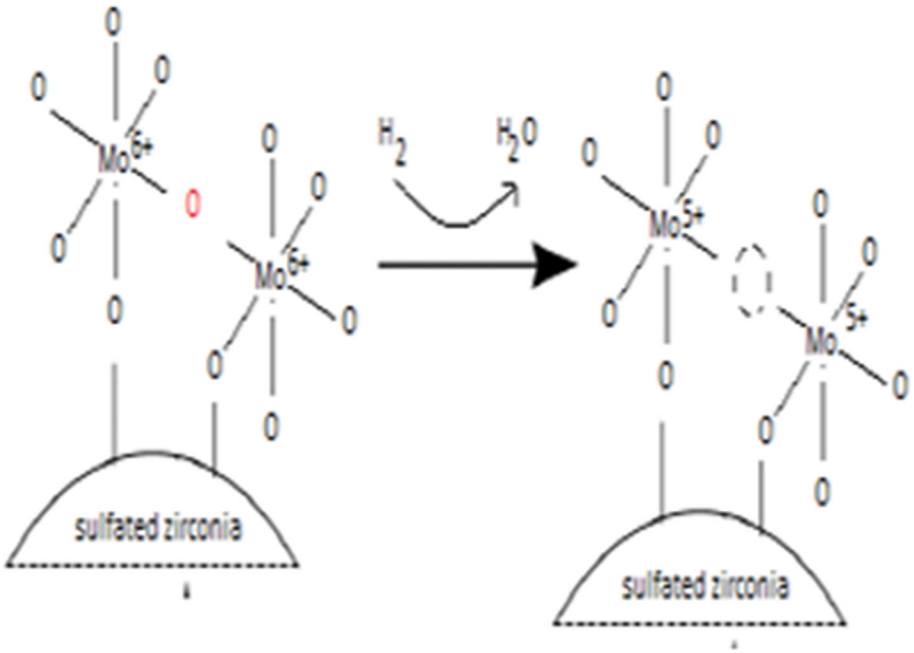

Fig. 9 Proposed pathway of interaction of octahedral molybdenum with H_2 and metallic sites reduction by dehydration

Table 1 Some catalytic activities of platinum or molybdenum sulfated zirconia in different conditions of *n*-hexane isomerization

Catalyst	Catalytic test conditions	Activity	Reference
ZS/Mo + Pt/Al_2O_3	$P = 1$ atm; H_2 flow = 30 mL/min; $P_{C6} = 0{,}027$ bar $T = 423$; 443; 473; 493	0.5; 3; 19; 27 10^{-7}mols^{-1} g^{-1}	Our catalyst
AZS + $PtAl_2O_3$	$T = 170$; 200; 220 °C; 20 torr of *n*-hexane diluted in total flow rate: 30 cc/min, $m = 200$ mg	106; 265; 340 10^{-8}mols^{-1} g^{-1}	[34]
XZS + $PtAl_2O_3$	$T = 170$; 200; 220 °C; 20 torr of *n*-hexane diluted in total flow rate: 30 cc/min, $m = 200$ mg	0.7; 18; 40 10^{-8}mols^{-1} g^{-1}	[34]
PtZS	$T = 150$ °C, $P = 2$ MPa, WHSV = 1.5 h − 1, H2/C6 = 3, $m = 0.5$ g	5 μmols^{-1} g^{-1}	[35]
PtAl-ZS	$T = 150$ °C, $P = 2$ MPa, WHSV = 1.5 h − 1, H2/C6 = 3, $m = 0.5$ g	3 μmols^{-1} g^{-1}	[35]
MoC_2/ZS	H_2 flow = 20 ml min^{-1}; *n*-hexane flow = 15.0 μL min^{-1}; GHSV 2.95 h^{-1}; $T = 450$ °C; $m = 0.2$ g	250 μmolmin^{-1} g^{-1}	[36]

Mo^{5+} on the zirconia surface. Reduction can spread over the surface. It means that electron moves from the Mo^{6+} cation to a neighboring Mo^{5+} cation by exchanging an electron. Proton moves at the same time to an O^{2-} anion attached to the adjacent Mo^{5+} cation. This motion can happen repeatedly. When the reduction moves away from the metal —support interface, the re-oxidized metal cation, at the periphery of the metal particle, can be reduced by another H atom. In the case of tetrahedral geometry (as mentioned in Fig. 8), molybdenum is easily reducible. However, proton–electron migration can be dependent of the metal lattice [36]. As observed on Fig. 9, reducibility of octahedral molybdenum is accompanied by a creation of irreversible oxygen vacancies. As we observed in our study, by calcination, the Mo–O distance distribution changes inducing a change in its coordination sphere and apparition of dimeric or polymeric Mo_xO_y species. This alteration is not favorable for the catalytic performances of this catalyst in the reaction of *n*-hexane isomerization [36].

4 Conclusion

In this study, we prepared an efficient catalyst of*n*-hexane hydro-isomerization. It consists on platinum supported on alumina mechanically mixed to sulfated zirconia doped with molybdenum and calcined at 673 K prepared by sol–gel method followed by drying in supercritical conditions of the propanol (536.6 K, 51 bar). We adjust preparation conditions to provide excellent catalytic properties:

– Catalytic activity, at 493 K, is about 2.7×10^{-7} mol s^{-1} g^{-1} which is almost 100 times faster than non-doped (ZS). Metal adjunction enhances selectivity of isomerization

products from 47 to 98%. Molybdenum, mainly on tetrahedral geometry, plays an important role in boosting (ZS) activity by favoring H_2 spillover and increasing acidity.
- Low calcination temperature (673 K) stabilizes molybdenum on tetrahedral geometry and favorites the dispersion of MoO_x on the surface of (ZS). Being easily reducible, they preserve sulfate sites and improve acidity by creation of protonic sites MoO_x–H_y^+. By increasing calcination temperature, we favorite the formation of octahedral molybdenum as MoO_3 species which are less active because of their hard reducibility and their inability to generate acid sites.
- Sol–gel method and supercritical drying favorites the development of specific surface area which is equal to 144 $m^2\ g^{-1}$ and the stabilization of ZrO_2 tetragonal phase that constitutes the requested phase in *n*-hexane isomerization.

Funding The authors have no relevant financial or non-financial interest to disclose.

Declarations

Conflict of interest The authors declare that they have no conflict of interest.

References

1. Barker, C.: Developments in Petroleum Science. Elsevier, Netherlands (1985)
2. OPEC report, WOO—Chapter 3—Oil demand (opec.org), 23/10/2022
3. Waquier, J.P.: Pétrole brut Produits pétroliers: Schémas de fabrication, Edition Techni (1994)
4. Naqvi, S.; Bibi, A.; Naqvi, M.; Noor, T.; Nizami, A.; Rehan, M.; Ayoub, M.: New trends in improving gasoline quality and octane through naphtha isomerization: a short review. Appl. Petrochem. Res. **8**, 131–139 (2018)
5. Speth, R.; Chow, E.W.; Malina, R.; Barrett, S.R.H.; Heywood, J.B.; Green, W.H.: Environ. Sci. Technol. **48**, 6561–6568 (2014)
6. Smolikova, M. D.; Kir'yanova, D. I.; Shkurenoka, V. A.; Bikmetovaa, L. I.; Belopukhova, E. A.; Yablokovaa, S. S.; Kazantseva, K. V.; Belyia, A. S.; Lavrenova A. V.; Kondrashevb, D. O.; Kleimenovb, A. V: Integrated processes of the reforming and isomerization of gasoline fractions for the production of environmentally friendly motor gasolines. Catal Indust. **14**(3), 268–282 (2022)
7. Saldana, D.A.; Starck, L.; Mougin, P.; Rousseau, B.; Pidol, L.; Jeuland, N.; Creton, B.: Flash point and cetane number predictions for fuel compounds using quantitative structure property relationship (QSPR) methods. Energy Fuels **25**, 3900–3908 (2011)
8. Dhar, A.; Vekariya, R.L.; Sharma, P.: Kinetics and mechanistic study of n-alkane hydroisomerization reaction on Pt-doped γ-alumina catalyst. Petrolium **4**, 489–495 (2017)
9. Ross, J.R.H.: Heterogeneous catalysis, fundamentals and applications. Elsevier, Netherlands (2012)
10. Garin, F.; Gault, G.: Mechanisms of hydrogenolysis and isomerization of hydrocarbons on metals. VIII. Isomerization of carbon-13 labeled pentanes on a 10% platinum-aluminum oxide sulphate. Am. Chem. Soc. 16, 4466–4476 (1975)
11. Keogh, R.A.; Srinivasan, R.; Davis, H.: Pt-SO_4^2–ZrO_2 Catalysts: the impact of water on their activity for hydrocarbon conversion. J. Catal **151**, 292–299 (1995)
12. Kumar, A.; Priyanka, Mangalam, J.; Yadav, V.; Goswami1, T.: Synthesis of sulfated zirconia catalyst using sol–gel technique for alkane isomerization. Reac. Kinet. Mecha. Catal. **135**, 1929–1944 (2022). https://doi.org/10.1007/s11144-022-02254-2
13. Anil, A.; Shah, R.B.; Misra, S.N.: Studies on surface characteristics and chemical resistance of zirconia nano coating developed on glazed ceramic wall tiles. In: International Conference on Advanced Nanomaterials & Emerging Engineering Technologies, pp 344–349 (2013)
14. Sekewael, S.J.; Pratika, R.A.; Hauli, L.; Amin, A.K.; Utami, M.; Wijaya, K.: Recent progress on sulfated nanozirconia as a solid acid catalyst in the hydrocracking reaction. Catalysts **12**, 191–197 (2022)
15. Mejri, I.; Younes, M.K.; Ghorbel, A.: Comparative study of the textural and structural properties of the aerogel and xerogel sulphated zirconia. J. Sol-Gel Sci. Technol. **40**, 3–8 (2006)
16. Ben Hammouda, L.; Ghorbel, A.: Influence of the zirconium precursor on the acidic and catalytic properties of sulphated zirconia catalysts prepared by sol–gel process. J Sol-Gel Sci Technol **89**, 543–552 (2019)
17. Colín, J.A.; Los Reyes, J.A.; Vázquez, A.; Montoya, A.: Pillar effects in MoS_2 catalysts supported on Al and Zr pillared clays in a hydrotreatment reaction: A preliminary study. Appl. Surf. Sci. **240**, 48–62 (2005)
18. Li, X.; Pang, J.; Luo, W.; Zaho, Y.; Pan, X.; Zhen, M.: Catalytic conversion of tetrahydrofurfuryl alcohol over stable Pt/MoS2 catalysts. Catal. Lett. **151**, 2734–2747 (2021)
19. Rojas, S.; Roble, M.; Morales-Ferreiro, J.O.; Diaz-Droguett, D.E.: Comparative study on the hydrogen storage capacity of crystalline and amorphous nanomaterials of MoO3: effect of a catalytic Pd capping. Ionics **24**, 3101–3111 (2018)
20. Raissi, S.; Younes, M.K.; Ghorbel, A.: Mesoporous aerogels and xerogls based on sulphated zirconia doped with cobalt as hexane isomerization catalysts. J. Mater. Sci. Eng. **4**, 105–111 (2014)
21. Raissi, S.; Kamoun, N.; Younes, M.K.; Ghorbel, A.: Effect of drying conditions on the textural, structural and catalytic properties of Cr/ZrO_2–SO_4: n-hexane conversion. React. Kinet. Mech. Catal. **115**, 499–512 (2015)
22. Thommes, M.; Kaneko, K.; Neimark, A.V.; Olivier, J.P.; Reinoso, R.F.; Rouquerol, J.; Sing, K.S.W.: Pure Appl. Chem. **87**, 1051 (2015)
23. Zemnukhova, L.A.; Panasenko, A.E.A.: A novel composite material based on antimony (III) oxide and amorphous silica. J. Solid State Chem. **201**, 9–12 (2013)
24. Moreno, J.A.; Poncelet, G.: n-Butane isomerization over transition metal-promoted sulfated zirconia catalysts: effect of metal and sulfate content. Appl. Catal. A **210**, 151–164 (2001)
25. Badoga, S.; Sharma, R.V.; Dalai, A.K.; Adjaye, J.: Hydrotreating of heavy gas oil on mesoporous zirconia supported NiMo catalyst with EDTA. Fuel **128**, 30–38 (2014)
26. Hirata, T.; Asari, E.; Kitajima, M.J.: Infrared and Raman spectroscopic studies of ZrO_2 polymorphs doped with Y_2O_3 or CeO_2. Solid State Chem. **110**, 201–207 (1994)
27. Cross, J.S.; Schrader, G.L.: Low pressure chemical vapor deposition of molybdenum oxides from molybdenum hexacarbonyl and oxygen. Thin Solid Films **259**, 5–13 (1995)
28. Thielemanna, J.P.; Resslerc, T.; Walterc, A.; Mullera, G.T.; Hess, C.: Structure of molybdenum oxide supported on silica SBA-15 studied by Raman, UV–Vis and X-ray absorption spectroscopy. Appl. Catal. A **399**, 28–34 (2011)
29. Castello, E.R.; Lopez, A.J.; Torres, P.M.; Jones, D.M.; Roziere, J.; Trombetta, M.; Busca, G.; Lenarda, M.; Storarod, L.: J. Solid State Chem. **175**, 159 (2003)

30. Spevack, P.A.; McIntyre, N.S.: J. Phys. Chem. **97**, 11020 (1993)
31. Phillippi, C.M.; Mazdiyasni, K.S.: Infrared and Raman spectra of zirconia polymorphs. J. Am. Ceram. Soc. **54**, 254–258 (1971)
32. Xiong P.; Gao, X.; Wang, W.; Zhang, J.; Song, F.; Zhang, Q.; Han, Y.; Tan Y.: Effect of calcination temperature on the structure and performance of molybdenum-tin catalyst for DME oxidation. J. Fuel Chem. Technol., **50**(1), 63–71 (2022)
33. Zhang, Z.; Zhang, Q.; Jia, L.; Wang, W.; Zhang, T.; Han, Y.; Tsubakiac, N.; Tan, Y.: Effects of tetrahedral molybdenum oxide species and MoOx domains on the selective oxidation of dimethyl ether under mild conditions. Catal. Sci. Technol. (2015). https://doi.org/10.1039/c5cy01569c
34. Mejri, I.; Younes, M.K.; Ghorbel, A.; Eloy, P.; Gaigneaux, E.M.: Comparative study of the sulfur loss in the xerogel and aerogel sulphated zirconia calcined at different temperatures: effect on n-hexane isomerization. Stud. Surf. Sci. Catal. **162**, 953–960 (2006)
35. Galadima, A.; Wells, R.P.K.; Anderson, J.A.: n-Alkane hydroconversion over carbided molybdena supported on sulfated zirconia. Appl. Petrochem. Res. **1**, 35–43 (2012)
36. Zhou, S.; Song, Y.; Zhou, X.: Study on the role of hydrogen in n-hexane isomerization over Pt promoted sulfated zirconia catalyst. Catal. Lett. (2022). https://doi.org/10.1007/s10562-022-04167-0
37. Prins, R.: Hydrogen spillover. Facts and fiction. Chem. Rev. **112**, 2714–2738 (2012)